

Observation of Network Dynamics of Ryanodine Receptors on Skeletal Muscle Sarcoplasmic Reticulum Membranes

Hongli Hu, Xing Meng

Wadsworth Centre, New York State Department of Health, Albany, New York, 12201, USA

This article is distributed under the terms of the Creative Commons Attribution Noncommercial License (CC BY-NC 4.0) which permits any noncommercial use, distribution, and reproduction in any medium, provided the original author(s) and source are credited.

Abstract

Rabbit muscle vesicles derived from sarcoplasmic reticulum were used as a material in studying networks of ryanodine receptors by cryo electron tomography. Three-dimensional analysis reveals the dynamical features of these networks. It was found that the connection angles were rotated along the transmembrane axis of ryanodine receptors. Majority of the connections was observed at domains 6/6 of ryanodine receptors while a small group of connections were showed at domains 9/10. The flexible rotation and connection shift seem to facilitate the extension of an annular network on the wall of the sarcoplasmic reticulum in a triad.

Key Words: Muscle, Network Dynamics, Ryanodine Receptors, Sarcoplasmic Reticulum

Eur J Transl Myol 2016; 26 (2): 101-108

Early observations of networks of ryanodine receptors (type I RyRs) of skeletal muscle was reported in 1984 from isolated guinea pig sarcoplasmic reticulum (SR) vesicles using the freeze-drying/replica and negative staining methods.¹ From toadfish muscle an indirect evidence for formation of RyR networks also was obtained in observations of the tetrad array of dihydropyridine receptors (DHPRs) that are thought of as the most important binding partners of RyRs.² The network of DHPR tetrads seen was extending to a whole T-tubule longitudinal region. A tetrad can precisely fit to a RyR. Upon the results, they described a triad model in which two rows of RyRs were inserted in the SR membrane along the longitudinal direction while RyR cytoplasmic domains spanned between transverse tubule (T-tubule) and the SR membranes. Groups of four DHPRs (the tetrads) were located on alternate cytoplasmic RyRs, extending to membranes of T-tubules.² By negative electron microscopy, early studies *in vitro* showed that the connection between the RyRs deviates from a checkerboard array.³ The repeat distance between two RyR centers was 31 nm. Further and comprehensive studies of 2D RyR crystals and modeling in the non-biological system were carried out,⁴⁻⁶ indicating that the binding sites between two adjacent RyRs are located at domains 6/6 with confirmation of the center-center distance (31 nm). Figs.1a and 1b (courtesy of Ferguson et al. 1984)¹ shows two structures of RyRs from vesicle samples. In Fig.1a, it presents a two-row pattern. For the network in Fig.1b it is difficult to determine if there are two or three rows of RyRs. It

appears that RyRs are arranged along two annular lines and perturbed. In general each RyR is oriented differently. The structure diversity observed can be explained as either structure distortion in specimen preparation or reflection of the true nature. Fig.1c (courtesy of Block et al 1988)² also briefly shows two rows of DHPR tetrads *in vivo*; noticeable, the RyR number should be the double of the tetrads on the alternate model in which DHPRs are arranged on every other RyRs. The information combined implies that RyRs *in vivo* should have a regulated array structure although the early observations in vesicles reveal not rigid patterns of distribution of RyRs.

In the model⁶ it describes the domains 6/6 connection between two adjacent RyRs with the center-center distance (31 nm) from the studies of RyR 2D crystals, which is close to 32 nm measured *in vivo*. The domains 9/10 connection was thought incorrect in considering that upon inversion the handedness of RyR in the model of domains 9/10 connection was reversed from left-handed pinwheel to right-handed pinwheel, which was contradictory to the handedness of the RyR projection map in the 2D array.⁶ The Yin's model requires that all RyRs have the uniform orientation and a constant center distance. In consequence, four particles form a closed square, which is the smallest unit in 2D space. A network can be thought of as an array of the unit finitely repeating periodically in a direction. In Figs.1a-1d, all RyR particles are at the "top-view" orientations. Indeed, there is the handedness problem in which cytoplasmic or

Network Dynamics of Ryanodine Receptors on Sarcoplasmic Reticulum

Eur J Transl Myol 26 (2): 101-108

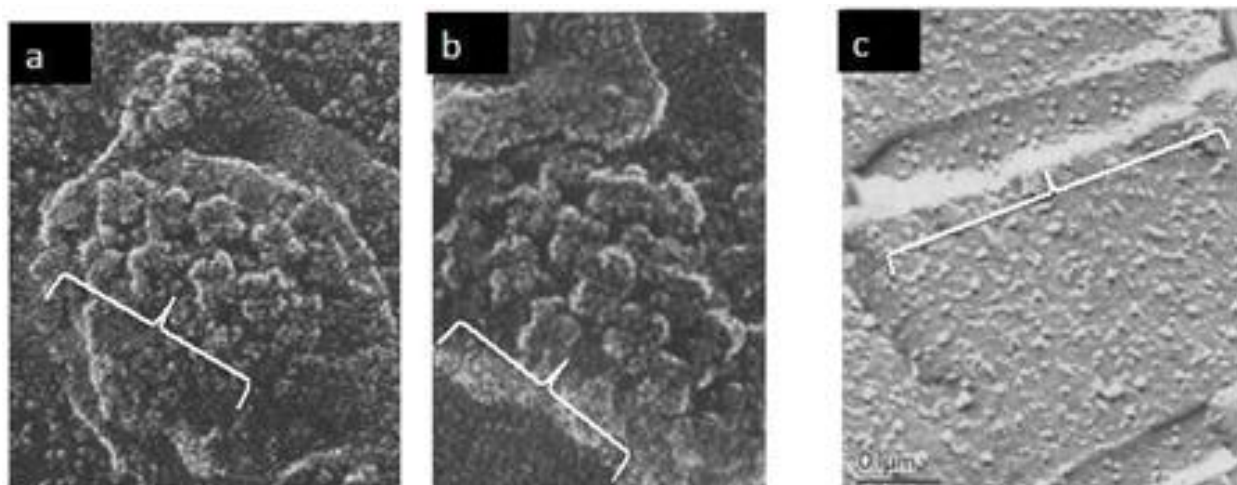


Fig 1. a. Two rows of RyRs from vesicles of guinea pig muscle; each RyR was seen with square shape and slightly disorientated (©Ferguson et al., 1984. Originally published in *The Journal of Cell Biology*. 99:1735-1742)¹; **b.** From the same resource as in “a.”, RyRs appear arranged with more dynamical perturbation. The pattern displayed is hardly determined with two or three rows (©Ferguson et al., 1984. Originally published in *The Journal of Cell Biology*. 99:1735-1742)¹; **c.** DHPR tetrad array observed in toadfish muscle along the long axis of the T-tubule; the RyR number must be double of the DHPR’s on the alternate model (©Block et al., 1988. Originally published in *The Journal of Cell Biology*. 107:2587-2600).²

transmembrane sides of a RyR may not be distinguishable in 2D images. The regular arrangement of RyRs and the size of the junctional gap are remarkably constant throughout the animal kingdom and in different fiber types,⁷ indicating that each RyR should have constant distance to membrane of a T-tubule. In nature, T-tubules are invaginations of the cell membrane and the invaginations form a series of tubes. Each T-tubule plus its two neighboring cisternae are considered a functional unit (the triad) wrapping around myofibrils in rings as shown in the reference Marieb EN, Hoehn J. 2012.¹⁸ This means that the network of RyRs should physically extend along an annular “racing track” (the wall of the SR membrane facing to the T-tubule membrane). The numbers of RyRs in networks for different skeletal muscles were measured showing lengths between 0.4-2 micrometers (estimated with diagonal length 41 nm multiplied by the pair number of RyRs.⁸ The profiles of triads along the long axis of T-tubules was recorded for the toadfish muscle as shown in Fig.1c and the image corresponds to the projection of a 90-degree flipped ring in which the length is a little less 500 nm.² In general the diameter of the myofibrils is less 2 micrometers, which means that the segment in Fig.1c is about 25% of the maximum diameter of myofibrils. All the information indicates significant curvatures of rings on which networks of RyRs are located. From the assessment upon previous work we can see that the ‘rigid’ 2D model of the network may not be reliable *in vivo* because it can extend only along a straight line that lies on the so-called longitudinal plane.⁶ There were yet

no reports of observations of RyR networks *in vivo*. Cryo electron tomography of vesicles offers two advantages; it builds 3D models of a structure, which eliminates the handedness problem when applying to RyRs; the cryo conditions can greatly minimize distortion of samples caused by drying and staining. SR vesicles from rabbits or rats have been used widely in physiological assessments for muscle studies because of integrity of the function domains on SR membranes.

In this paper, we are reporting our experimental observations of RyR distributions on SR vesicles by cryo electron tomography and describing the network dynamics discovered.

Materials and methods

SR-derived vesicles were isolated as described previously.⁹ To prepare specimen grids for cryo-TEM 4μL aliquot of the vesicles was applied to 200-mesh home-made holey grids without thin carbon films (i.e., the over-hole method). The grids were blotted with Whatman #540 filter paper, and plunged into liquid ethane using Gatan CP3. Colloidal gold (10 nm) particles were added as fiducial markers into buffers. It was found that vesicle samples must be stored with a buffer containing 10% sucrose and it can take instant dilution to 2.5% before blotting and plunging. The grids using samples stored at -80°C with less than 10% sucrose showed great decrease of the number of vesicles. In addition, we employed a technique to improve over-hole ice layers. It made blotting more

Network Dynamics of Ryanodine Receptors on Sarcoplasmic Reticulum

Eur J Transl Myol 26 (2): 101-108

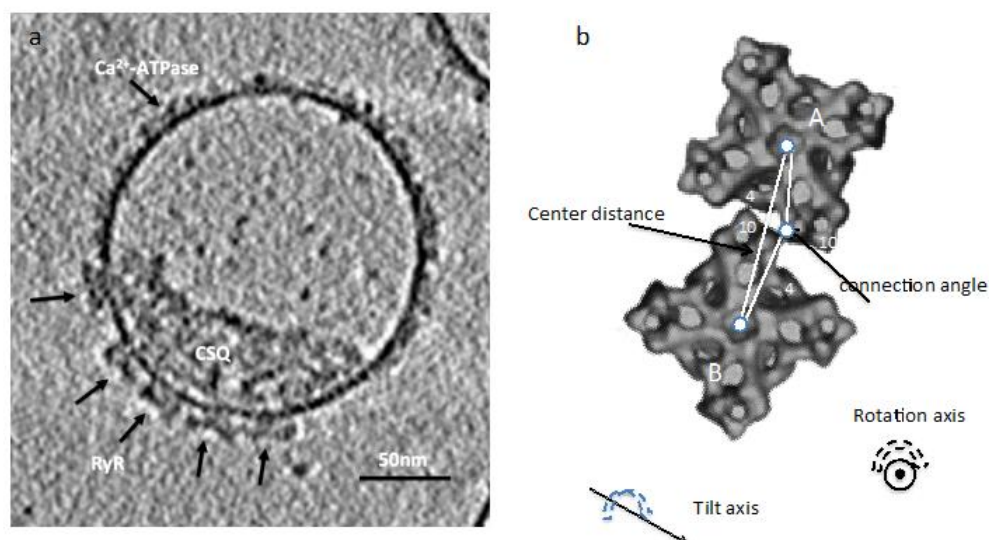


Fig 2. *a.* A section of a tomogram obtained by Cryo EM showing good integrity of RyRs with SR membrane and close association with CSQ; A few RyR particles were distributed on the spherical surface; *b.* Diagram of definition of the linkages parameters used in statistical measurement; additionally, it shows the maximum rotation clockwise leading to the contact of domains 10/4.

“gentle” in water absorption, producing more useful areas. The idea was to let filter paper slowly wet by moistening it in a sealed container at 100% humidity without touching the water surface for 24 hours (a small dry petridish with filter paper pieces is sealed in a large petridish with some water in the large petridish bottom). The paper-wetting technique is more useful for buffers including sucrose (up to 10%) meanwhile the thin carbon films are used in cryo TEM. Tilt series (-60° to 60°) were collected at $2^\circ/1^\circ$ intervals at an electron dose of $1\sim 0.5$ e/ \AA^2 per image (60 e/ \AA^2 total estimated dose per set). Data were collected using a FEI TF20 and a JEOL JEM-3200 transmission electron microscopes operated at 200 kV and 300kV separately. For both microscopes the defocuses had a range from -5 to $-12\mu\text{m}$. TF20 is equipped with TVIPS 415 CCD, JEOL 3200 with TVIPS 416 CMOS cameras. Automated data collection was performed with SerieIEM.²⁹ The pixel size 0.58 nm at 2k by 2k setting (binning=2) was used to collect data for CCD; for CMOS it was 0.57 nm. Tomograms were calculated by IMOD¹⁰ with further binned (pixel-size= 1.16 nm). Analysis of 3d volumes was performed by Chimera¹¹ and Spider.¹²

Results

Although over 300 datasets were collected and most of them were used in creating corresponding tomograms, only a dozen of tomograms have shown the resolved 3D RyR network structure. In general cases, the regions including many vesicles with interested structure showed poor image contrast. RyRs were identified in tomograms. The signal/noise ratio is the key for the

structure to be extractable. The thick ice-layers and sucrose in the buffer are the reason for poor image contrast. When diluting the sucrose to zero level in the buffer the number of vesicles was greatly decreased and the structure damage of vesicle was enhanced. Most used tomograms had a thickness below 160 nm. In overall, the structure of vesicles is consistent with the early work,¹³ showing a good association between RyR and calsequestrin (CSQ, the Ca²⁺ storage protein). The distortion of the triad structure observed demonstrates that vesicles are better used to study the proteins on SR membranes because of well-preserved integrity. As a typical structure, a slice of tomogram from a vesicle is shown in Fig.2a. In the configuration, the transmembrane units of RyRs are inserted in the SR membrane. RyR particles are at “side-view” orientation and the sides of thin sheets of cytoplasmic RyRs are visible as marked. In the luminal area of the SR membrane, CSQ clusters are closely associated to RyRs. Ca²⁺-ATPase is presented as indicated in Fig.2a, which are not associated with CSQ.

Consecutive sections of a tomogram are shown in Fig.3a, presenting a group of top-view RyR particles connected with each other. These RyR particles appear distributed on the curved surface. Each of RyRs has different orientation in a sense of rigidity. In the model of RyR network described In the model⁶ three points (two centers of RyRs and the connection point at domains 6/6) are collinear. Our observations show that the connection points are not on the lines between two adjacent RyR centers. This feature can only be determined through 3D maps because of curvature of

Network Dynamics of Ryanodine Receptors on Sarcoplasmic Reticulum

Eur J Transl Myol 26 (2): 101-108

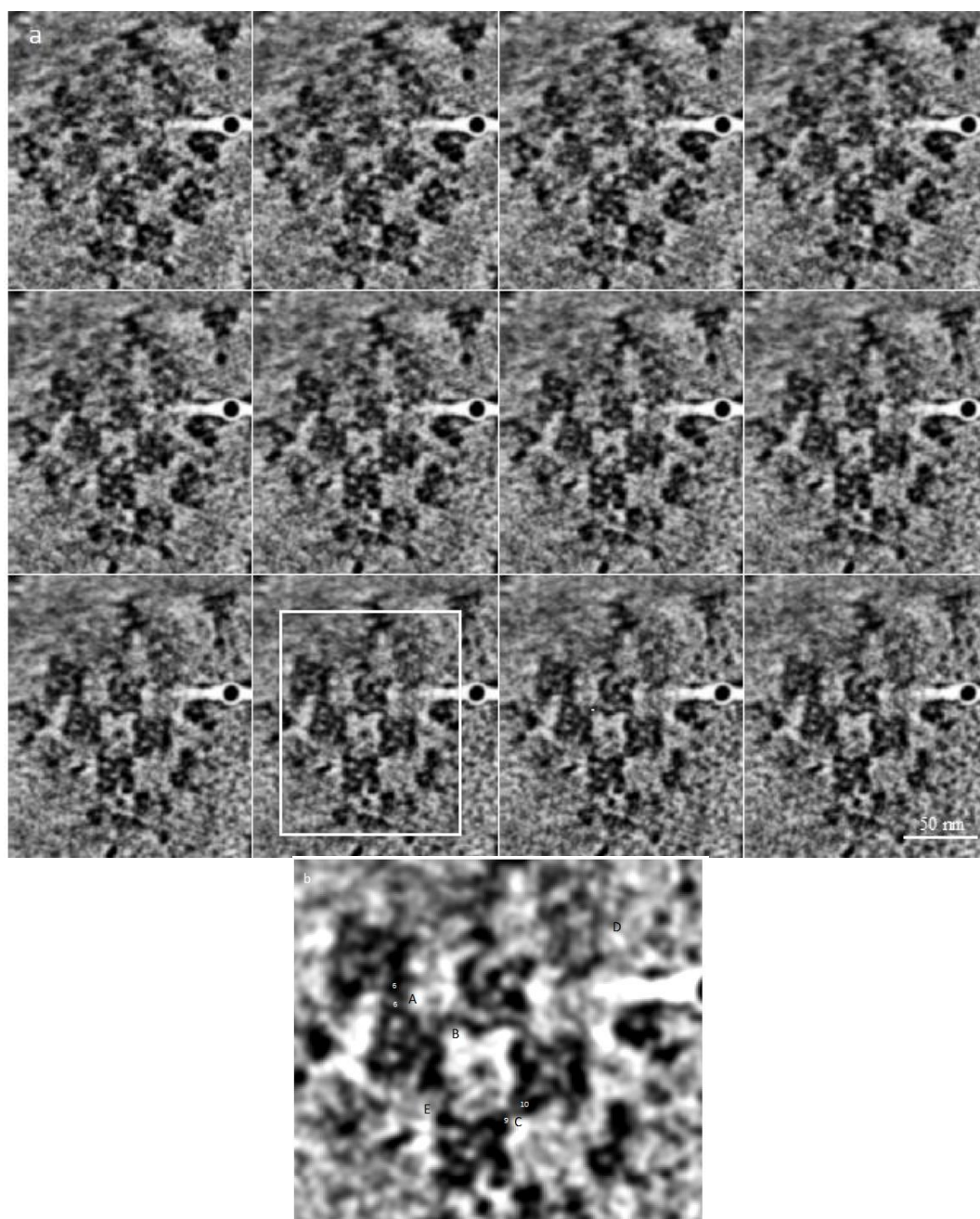


Fig 3. *a. Consecutive sections of a tomogram showing basically two-row of RyRs with clearly linkage elongation and the particles are not co-planar; as similar with figure 1b, there are some particles off the two-row axis; b. The squared section in Fig.3a; position “A”, domains 6/6 connection; position “B”, domains 6/6 connection with linkage elongation in which there is mass contrast between the two adjacent RyRs; position “C”, domains 10/9 connection.*

vesicles. Obviously this is the consequence of the observed angular rotation between the adjacent RyRs. In addition, there were connections observed through domains 9/10 (connection shift). Extended mass domains from connections either 6/6 or 9/10 (“linkage elongation”) were also observed. Fig.3b is the enlargement of the section (square marked) in Fig.3a. Position “A” presents the connection with domains 6/6

without elongation. At position “B” the two adjacent RyR squares are connected with an extended domain in between. Position “C” shows a connection of domains 9/10, connection shift. The center distances for a pair of adjacent RyRs appear longer when having the linkage elongation or/and connection shifts. The structure at position “D” was not well resolved. Its brief triangle shape indicates that there is a high tilt

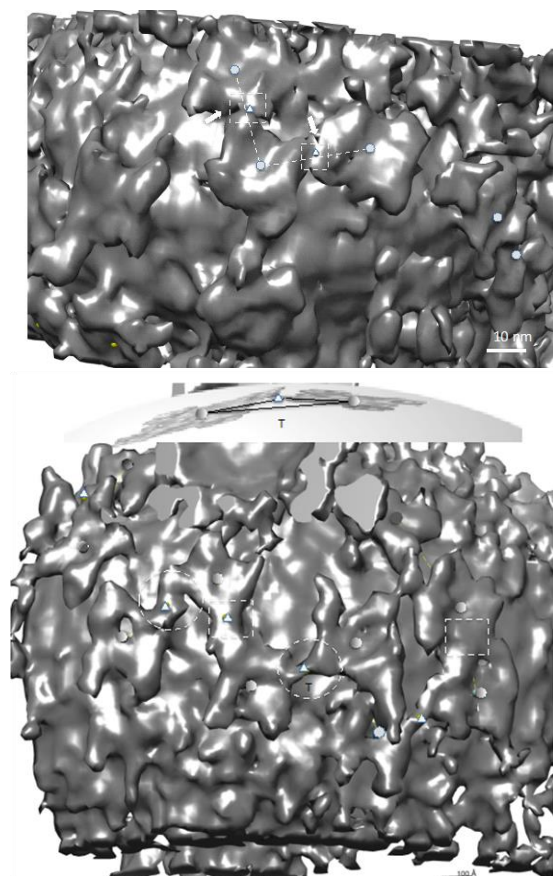


Fig 4. *The segmented structure from tomograms. a. Three particles show domains 6/6 connection (dash squares) and about 31 nm linkage distances; b. The circles mark 10/9 connection, accompanying with linkage elongation; here briefly is a two-row network. The diagram on top describes the configuration marked with “T”.*

with other nearby RyRs, which may imply a RyR3.^{14,15} Interestingly, there is a pair of neighboring RyRs without physical connection at position “E”. The structure described in Fig. 3 represents the typical and general pattern of observed network, which is confirmed by those with side-view orientations. For the quantitative assessment of the network morphology, we define the center distance as the straight line between two adjacent RyR particle centers. Precisely, three points (two RyR centers and one connection point) form a triangle as described in Fig.2b where the obtuse angle is defined as the connection angle. In the 2D network model, the triangle becomes a line and the connection angle is 180 degree. Using this plane geometry we can simplify the measurement on required parameters meanwhile preserving the equivalency of measurement to all vesicles. The profile of rotation/tilt angles and center distances were measured on the scheme in Fig.2b. It shows that two adjacent RyRs, “A” and “B”, can be

rotated with each other along the axis (the parallel to the normal of paper), which is parallel to the transmembrane axis. The domains 6/6 will keep connected. The limitation for the rotation will be reached when the domain 10 of RyR “B” touches domain 4 of RyR “A”, verse visa (domain 4 of RyR “B” touches domain 10 of RyR “A”). In the situation the two adjacent RyRs have two connection points. Another possible angular variation is tilted along the axis lying on the paper plane indicated in Fig.2b, which is called the tilt axis. Hence, the two components of rotation and tilt represent all possible angular movement. When the rotation angle is equal to 180, two adjacent RyRs are at the identical orientation (without tilt), which is the case described in the model⁶. The maximum rotation (a touch with domains 10/4 connection) is identical to connection angle of about 155 degree. Mostly, the observations showed that each RyR had different orientations. There were no collinear three points (two centers and one connection point), and no closed squares formed by four RyRs. The tomogram in Fig.3 with the top-view RyRs includes only parts of RyR domains.

The accurate measurement requires positioning the centers of structure motifs, which needs to perform it with 3D tool as Chimera.¹¹ The tomograms with side-view networks including whole masses of RyRs as shown in Fig.2a were explored to obtain the statistical profile. Fig.4a shows the typical segmented RyR particles used in measurement. The small balls are used to mark the centers of RyR particles while the small triangles for marking the connection points. The dash squares mark the domains 6/6 connections. The arrows indicate the contacts of domains 10/4. In Fig.4b, it shows a network on the spherical surface including some linkage elongations, being connected at either domains 6/6 or domains 9/10 (marked with the dash circles). It must be noted that the small triangle (marked with a “T” appears on the line of center distances in Fig.4b. This is because the center distance line is below the triangle in 3D perspective view. The diagram at the top-right of Fig.4b explains the configuration. The measured center distances can be classified into two groups in the total number of measurement, 39 pairs; one group that includes 28 center distances has the average of 31 ± 1.2 nm and another group has 11 center distances, and the average of 36 ± 1.5 nm, which include six connection-shifts. Only one pair that has no elongation belongs to the shifted, which means the connection shift is correlated with linkage elongation. The ratio between 9/10 and 6/6 is about 18%. The connection angles show uncorrelated scattering with both center distances and diameters of vesicles; the angular variation ranges from 140 to 170 degree with the average of 158 degree, which is close to the angle (155 degree), the maximum rotation model described in Fig.2b.

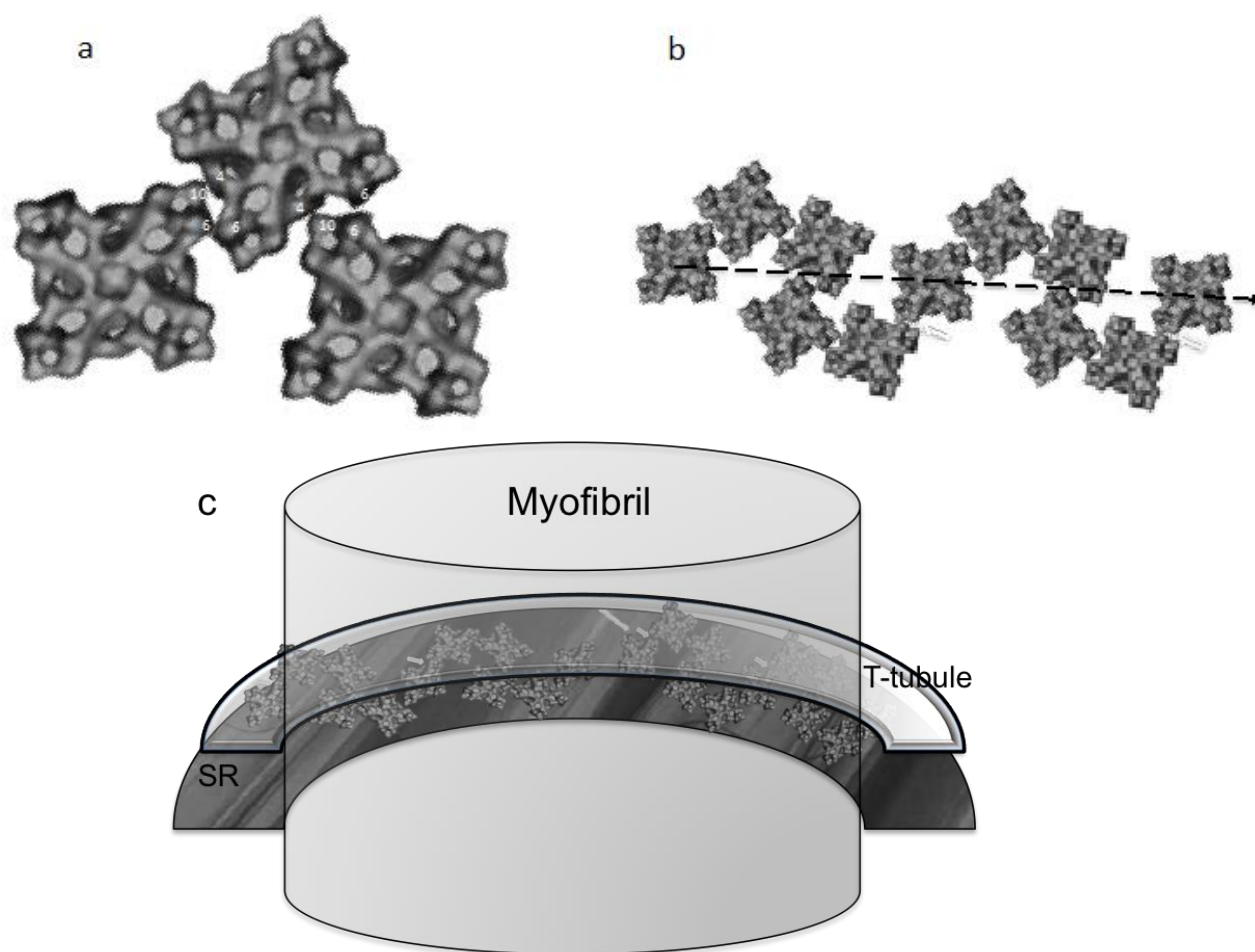


Fig. 5 *a. Three RyRs with three different orientations form the basic unit in which the adjacent pair has domains 6/6 and domains 10/4 connections as indicated in Fig.2b; b. A model network extended along a longitudinal plane built from the unit in "a", showing domains 9/10 is inevitable for extension; c. RyRs on a triad (up SP membrane and DHPR are ignored), an annular "racing track".*

Discussion

The measured connection angles include two angular components (rotation and tilt, Fig.2b). The results show the dominance of rotation rather than the tilt. The array model based on the 2D crystal observation in requires that each RyR has the uniform orientation,⁶ which can extend themselves along an axis in formation a tow-row network in a triad. This creates a pattern with rigidity in center distance and connection angle. The observed RyR network in the vesicles by Cryo EM shows that each particle is orientated non-uniformly. In average, the connection angles are varied around the maximum limit of rotation. In overall, it appears that each particle can be flexibly orientated within the angular limit and has a constant center distance (31 nm), which is the main profile of the network. In addition, observations showed that there were neighboring particles without physical touches. This angular flexibility seems a measure to

facilitate the extension of RyR network annularly. The angular rotation observed in vesicles presets the inevitability. In addition, the angular flexibility dissolves the collinear among three connection points and makes it rare to have closed units.

As a simulation, we built a model network upon maximum angular rotation assuming the network with a zero curvature along the longitudinal for simplicity. Also for simplicity we are not considering the elongation yet. Fig.5a presents a basic pattern of the model network and it includes three particles at three different orientations respectively. For the three particles we set the connection angles with the configuration at which there are two contact points for the adjacent pairs with the maximum rotation. Assuming that two connection points may be more stable than one, the configuration in Fig.5a is the only arrangement for three particles, which is supported by

Network Dynamics of Ryanodine Receptors on Sarcoplasmic Reticulum

Eur J Transl Myol 26 (2): 101-108

experimental evidence as shown in Figs.3c and 4. More important, the connection angles are 155 degree that is close to the average rotation measured (158 degree). In extending the model network along a longitudinal axis, RyR particles that have one of the three orientations, have been arranged, resulting in a model network as shown in Fig.5b. The path of the array extension appears zigzag or wavy. The arrows indicate the domains 9/10 connections or connection shift. In the modeling (excises) it would have the “dead-lock” to extend the network if not imposing the connection shifts (domains 9/10 connections). In the two conditions (maximum rotation and extension along the longitudinal direction) it “forces” taking alternative measure in angular configuration. This means that the connection shift may be a tool to mediate the network extension physically. Practically, each RyR can have an angular position between two maximum rotations and a network could be formed annularly. We can imagine an annular RyR “racing track” by adjusting angular positions of RyRs as shown in Fig.5c. Rotations of RyRs should be the control parameter to decide the curvature of a network. As well, the pattern of the model network presents itself as a look of pseudo three-row for which we puzzled in explaining the image as shown in Fig.1b. The above simulation does not only create the similar morphology with experiments, but also it reveals a possible reason to have connection shift.

The linkage elongation is correlated with vesicle bending as shown in Fig.4b. It is possible that in connection domain (domains 6, 9 and 10) exists some flexibility in a small length range. We wonder if the curvature of the resident plane of RyRs is small or ignorable *in vivo*. If so, the elongation is an artificial effect. However, the sizes of vesicles were not found being correlated with the elongation. The wrapping SR membrane during the isolation process could be equivalent to wrapping an adhesive sphere with an elastic sheet.¹⁶ If the sizes of spheres are much larger than the size of the sheet (here RyR particle), the strain on the sheet because spherical surface bending is ignorable.¹⁶ More importantly, only the transmembrane unit of a RyR is actually inserted to the SR membrane, which has 44% of RyR handle size. For the smallest vesicle (120 nm), it has a ratio less than 3% between the transmembrane size and vesicle girth. It is likely that both the artificial and natural bending exist. In routine, the muscle contraction involves that the thin filaments slide past the thick filaments; the thick filaments pull the thin filaments toward the center of the sarcomere; overlap between the myofilaments increases as the thin filaments slide they pull the Z discs toward each other and the sarcomere shortens; all of the sarcomeres along the myofibril shorten and all of the myofibrils within the muscle fiber shorten. This is so called “sliding filament model of contraction”. There is an optimal length-tension relationship when the muscle is slightly stretched and there is slight overlap between the myofibrils. These longitudinal activities of

myofibrils unavoidably bring a force along the axis of myofibrils on both the T-tubule and SR membrane walls that have the normal parallel to the axis. Elastic wrinkling on the membranes could be the consequence of those activities.

Therefore, an annular “racing track” with a low-curvature wavy surface is a reliable model of RyR residence. An outcome to confirm this can come from the emerging techniques of cryo focused-ion beam milling and electron tomography,¹⁷ which allows to obtain 3D structure of native triads. Vesicles are not used as a model to describe triads accurately *in vivo*. However, dynamics of RyR networks from tomograms of vesicles may reveal the mechanism that sets up the network *in vivo*.

Acknowledgement

This work was supported by NIH grants R01 AR40615. Ms. Ying Liu contributed to the development of wet paper methods for making cryo grids with buffers including sucrose.

Conflict of Interest

The authors declare no conflict of interests.

Corresponding Author

Xing Meng, Wadsworth Centre, New York State Department of Health, Albany, New York, 12201, USA. Email: xmeng101@gmail.com

References

1. Ferguson DG, Schwartz HW, Franzini-Armstrong C. Subunit structure of junctional feet in triads of skeletal muscle: A freeze-drying, rotary-shadowing study. *J Cell Biol* 1984;99:1735-42.
2. Block BA, Imagawa T, Campbell KP, Franzini-Armstrong C. Structural evidence for direct interaction between the molecular components of the transverse tubule/sarcoplasmic reticulum junction in skeletal muscle. *J Cell Biol* 1988;107:2587-600.
3. Saito A, Inui M, Radermacher M, Frank J, Fleischer S. Ultrastructure of the calcium release channel of sarcoplasmic reticulum. *J Cell Biology* 1988;107:211-9.
4. Yin CC, D'Cruz LG, Lai FA: Ryanodine receptor arrays: Not just a pretty pattern? *Trends Cell Biol* 2008;18:149-56.
5. Yin CC, Lai FA. Intrinsic lattice formation by the ryanodine receptor calcium-release channel. *Nat Cell Biol* 2000;2:669-71.
6. Yin CC, Blayney LM, Lai FA. Physical coupling between ryanodine receptor-calcium release channels. *J Mol Biol* 2005;349:538-46.
7. Franzini-Armstrong C, Nunzi G. Junctional feet and particles in the triads of a fast-twitch muscle fibre. *J Muscle Res Cell Motil* 1983;4:233-52.

Network Dynamics of Ryanodine Receptors on Sarcoplasmic Reticulum

Eur J Transl Myol 26 (2): 101-108

8. Franzini-Armstrong C, Protasi F, Ramesh V. Shape, size, and distribution of Ca^{2+} release units and couplons in skeletal and cardiac muscles. *Biophys J* 1999;77:1528-39.
9. Saito A, Seiler S, Chu A, Fleischer S. Preparation and morphology of sarcoplasmic reticulum terminal cisternae from rabbit skeletal muscle. *J Cell Biol* 1984;99:875-85.
10. Kremer JR, Mastrorade DN, McIntosh JR. Computer visualization of three-dimensional image data using imod. *J Struct Biol* 1996;116:71-76.
11. Pettersen EF, Goddard TD, Huang CC, et al. Ucsf chimera-a visualization system for exploratory research and analysis. *J Comput Chem* 2004;25:1605-12.
12. Beard NA, Laver DR, Dulhunty AF. Calsequestrin and the calcium release channel of skeletal and cardiac muscle. *Prog Biophys Mol Biol* 2004;85:33-69.
13. Wagenknecht T, Hsieh CE, Rath BK, Fleischer S, Marko M. Electron tomography of frozen-hydrated isolated triad junctions. *Biophys J* 2002;83:2491-2501.
14. Protasi F, Takekura H, Wang Y, et al. Ryr1 and ryr3 have different roles in the assembly of calcium release units of skeletal muscle. *Biophys J* 2000;79:2494-508.
15. Flucher BE, Conti A, Takeshima H, Sorrentino V. Type 3 and type 1 ryanodine receptors are localized in triads of the same mammalian skeletal muscle fibers. *J Cell Biol* 1999;146:621-30.
16. Hure J, Roman B, Bico J. Wrapping an adhesive sphere with an elastic sheet. *Phys Rev Lett* 2011;106:174301. Epub 2011 Apr 25.
17. Wagenknecht T, Hsieh C, Marko M. Skeletal muscle triad junction ultrastructure by focused-ion-beam milling of muscle and cryo-electron tomography. *Eur J Transl Myol* 2015 Jan 15;25:4823. doi: 10.4081/ejtm.2015.4823. eCollection 2015 Jan 7. Review.
18. Marieb EN, Hoehn J. *Human Anatomy & Physiology*, 9th ed. New York, Pearson, 2012, p. 291.